Appl. Phys. B 72, 157–162 (2001) / Digital Object Identifier (DOI) 10.1007/s003400000441

Applied Physics B
Lasers
and Optics

Green up-conversion of Er^{3+} in $KGd(WO_4)_2$ crystals. Effects of sample orientation and erbium concentration

M. Rico[1], **M.C. Pujol**[2], **F. Díaz**[2], **C. Zaldo**[1,*]

[1] Instituto de Ciencia de Materiales de Madrid, Consejo Superior de Investigaciones Científicas, Cantoblanco 28049 Madrid, Spain
[2] Laboratori de Física Aplicada i Cristal.lografia, Universitat Rovira i Virgili, 43005 Tarragona, Spain

Received: 4 July 2000/Published online: 22 November 2000 – © Springer-Verlag 2000

Abstract. Pumping with infrared light resonant to the energy position of $^4I_{11/2}$ and $^4I_{9/2}$ multiplets respectively has excited green up-conversion of Er^{3+} in $KGd(WO_4)_2$ single crystal. At room temperature the maximum green-emission intensity is achieved by pumping with light polarized parallel to the C_2 symmetry axis of the crystal ($//p$) at 981 and 801.5 nm, while pumping with light parallel to the principal m axis ($//m$) has maximum up-conversion at 978.2, 806 and 800 nm. The emission is weakly polarized. The maximum of the emission peaks at 547.8 nm if the light is analyzed parallel to the C_2 axis or at 552.4 nm for light perpendicular to it. The largest emission intensity was achieved with an erbium concentration about 3×10^{20} cm^{-3}. A schematic model of the up-conversion process is suggested.

PACS: 42.70-Hj; 78.55-Hx

$KGd(WO_4)_2$ single crystal (hereafter KGW) is a novel laser matrix that is receiving a lot of attention due to the high efficiency of the 1.06 μm Nd^{3+} emission [1]. Further interest is due to the coupling of the laser emission with optical phonons of the lattice, giving rise to self-induced frequency shifting [2, 3].

The Er^{3+} spectroscopy in this lattice has been described in a recent work [4]. Figure 1 summarizes the Er^{3+} energy levels for reference. However, polarization effects were not considered and only samples with a moderate erbium concentration ([Er] $< 5.5 \times 10^{20}$ cm^{-3}) were used, even though Er^{3+} can completely replace Gd^{3+} [5]. The photoluminescence of the $^4S_{3/2}$ multiplet excited by ground-state absorption was described, but cooperative excitation mechanisms (such as up-conversion) were ignored.

Up-conversion processes give the opportunity to produce visible radiation by pumping with infrared light. Green $^4S_{3/2} \rightarrow {}^4I_{15/2}$ Er^{3+} up-conversion emission can be achieved under different pumping conditions. Using a single wavelength, the up-conversion process can be started by pumping the $^4I_{13/2}$, $^4I_{11/2}$, $^4I_{9/2}$ or $^4F_{9/2}$ multiplets with $\lambda \approx$ 1.51 mm [6], $\lambda \approx 980$ nm [7, 8], $\lambda \approx 810$ nm [8] and $\lambda \approx 640$ nm [9] respectively. Dual-wavelength pump schemes can also be used to enhance the excitation of the intermediate state [10]. Some of these excitation channels allow the use of diode lasers for pumping in order to realize all-solid-state visible lasers if the efficiency of the process was optimized.

In fact, Er^{3+} laser emission via up-conversion has been demonstrated at room temperature in other matrices: single-wavelength pumping at $\lambda \approx 810$ nm is possible [11], but it

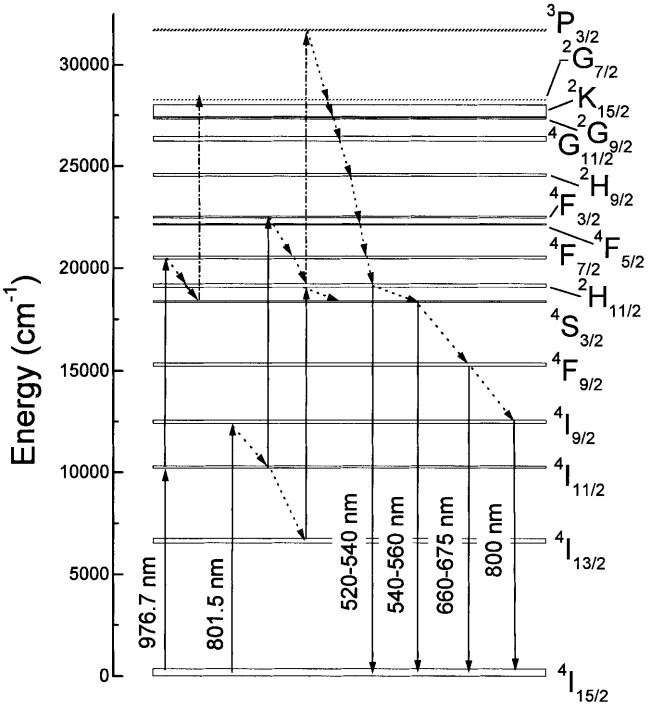

Fig. 1. Energy-level diagram of the Er^{3+} multiplets involved in up-conversion processes in KGW. The $^2G_{7/2}$ and $^2P_{3/2}$ energy positions (*dashed lines*) are taken from Er^{3+} in LaF_3. *Continuous arrows* indicate pumping channels for the up-conversion. *Dashed arrows* indicate non-radiative transitions and *dot–dashed arrows* are possible excitation channels only operative in the lowest concentration sample, [Er] $= 1.1 \times 10^{20}$ cm^{-3}

*Corresponding author. (E-mail: cezaldo@icmm.csic.es)

has a high laser threshold because of the very weak ground-state absorption of the $^4I_{9/2}$ multiplet; simultaneous pumping to the $^4F_{9/2}$ multiplet with a krypton laser helps to reduce this laser threshold [8, 12]. Single-wavelength pumping of the $^4I_{11/2}$ multiplet ($\lambda \approx 974$ nm) is also feasible [13], and in this case the energy transfer from Yb codopants improves the pumping efficiency.

In this work, we are concerned with single-wavelength excitation of the $^4I_{11/2}$ and $^4I_{9/2}$ Er^{3+} multiplets in KGW. Since the spectroscopic polarization rules of this monoclinic crystal are not well established, we have determined the pumping conditions (with particular emphasis on polarization) and erbium concentration leading to maximum output of up-conversion emission at room temperature.

1 Experimental techniques

KGW has a monoclinic crystallographic structure with lattice parameters $a = 10.652$ Å, $b = 10.374$ Å, $c = 7.582$ Å, $\beta = 130.80°$. The principal axis p of the indicatrix with smallest refractive index is parallel to the crystallographic b axis. The two other principal axes, m and g, lie in the crystallographic ac plane. The g axis forms an angle with the crystallographic c axis of 21.5° in the clockwise direction when looking from the positive end of the b axis [4]. The m axis is orthogonal to the g one. The samples used in our study were prisms cut with the faces perpendicular to the three principal axes.

KGW single crystals were grown by the top-seeded solution-growth slow-cooling method. Details of the crystal growth have been given previously [4]. The Er concentration in the crystal ([Er]) was determined for all samples in a relative manner by electron-probe microanalysis (EPMA) using Cameca Camebax SX 50 equipment, and quantified to an absolute value by particle-induced X-ray emission (PIXE) measurements made in selected samples. In our previous work [4] the concentrations determined by PIXE provided a better agreement for the calculated erbium spectroscopic parameters. The relation between both concentrations is $[\mathrm{Er}]_{\mathrm{PIXE}} = 2.2[\mathrm{Er}]_{\mathrm{EPMA}}$; this gives an idea of the uncertainty in the measurements. In this work we will use the concentration determined by PIXE; therefore, the absorption and emission cross sections calculated should be considered as low limits.

Up-conversion emission was excited with a Ti–sapphire laser and the emitted light was analyzed using a Spex 340-E spectrometer ($f = 34$ cm) and detected with a photomultiplier and a lock-in. The pumping wavelength was calibrated with a Burleigh wavemeter, model WA-2500, with an accuracy of ± 0.1 nm. Optical absorption spectra were recorded with a Cary 5E spectrophotometer.

In order to make comparative luminescence experiments between samples with different erbium concentrations and different polarization configurations of the pump and emitted light, the beam of the Ti–sapphire laser remains stationary and its polarization state is changed with a $\lambda/2$ plate. The unexpanded beam propagates through the sample and the image of the first 4 mm of the beam path as it enters the sample is focused on the spectrometer. The laser intensity is regulated to maintain constant the excitation intensity on the sample independently of the polarization configuration. A Glan–Taylor polarizer is used to analyze the emitted light; the principal axis of this analyzer is always at the same position with regard to the grating of the spectrometer. The polarization configuration is selected by changing the sample orientation.

For lifetime measurements the photoluminescence of the $^4S_{3/2}$ level was excited at $\lambda = 543.8$ nm with a Spectra Physics optical parametric system, model MOPO-730. The $^4S_{3/2} \rightarrow {}^4I_{13/2}$ emission at $\lambda = 862$ nm was analyzed with a Spex 500M spectrometer and the signal was detected by a GaInAs photomultiplier and a Tektronix oscilloscope.

2 Experimental results

Figure 2 shows the room-temperature ground-state optical absorption (GSA) coefficient, α_{GSA}, of the $^4S_{3/2}$, $^4I_{9/2}$ and $^4I_{11/2}$ multiplets of Er^{3+} in KGW recorded with light polarized parallel to the three principal axes. It is worth noting that the intensity of the GSA is strongly sensitive to the polarization of the light. Moreover, the peak intensity of the GSA corresponding to $^4I_{9/2}$ is only a factor 0.5 weaker than that measured for the $^4I_{11/2}$ multiplet. This is a remarkable difference with the spectroscopic properties of Er in other crystals used for up-conversion, for instance in $YLiF_4$ [11] and $LiNbO_3$ [14], for which the GSA intensity ratio between $^4I_{9/2}$ and $^4I_{11/2}$ multiplets is about $0.1 - 0.15$. The Er^{3+} GSA in KGW roughly scales linearly the Er concentration; the inset of Fig. 2 shows this linearity. Table 1 gives the value of the ground-state absorption cross sections, $\sigma_{\mathrm{GSA}} = \alpha/[\mathrm{Er}]$, for some relevant wavelengths.

The 300 K emission induced by up-conversion exhibits two complex bands in the green region, which are illustrated in Fig. 3. In addition to these bands, much weaker $^4F_{9/2} \rightarrow {}^4I_{15/2}$ and $^4I_{9/2} \rightarrow {}^4I_{15/2}$ emissions were also observed in the 660–675-nm and 780–815-nm regions respectively. The latter are not shown for the sake of brevity. No emission was observed for wavelengths shorter than 500 nm. The shape of the green-emission spectra presented in Fig. 3 is independent of which one of the $^4I_{11/2}$ or $^4I_{9/2}$ multiplets is excited. The complex band peaking at shorter wavelength corresponds to the $^2H_{11/2} \rightarrow {}^4I_{15/2}$ decay and that peaking at longer wavelength to the $^4S_{3/2} \rightarrow {}^4I_{15/2}$ decay. In the spectra

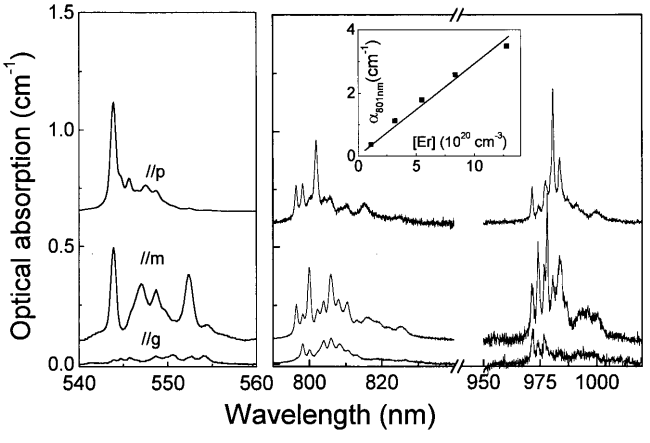

Fig. 2. 300 K polarized ground-state absorption of KGW:Er, [Er] = 1.1×10^{20} cm^{-3}, corresponding to $^4I_{15/2} \longrightarrow {}^4S_{3/2}$, $^4I_{9/2}$ and $^4I_{11/2}$ transitions. The *inset* shows the relationship between the GSA coefficient at 801.5 nm and the erbium concentration determined by PIXE

Table 1. Room-temperature ground-state absorption, σ_{GSA}, and emission, σ_{EMI}, cross sections for the relevant wavelengths of several Er^{3+} multiplets in KGW

	Polzn, λ(nm)	$\sigma_{GSA}(10^{-21}\ cm^2)$	$\sigma_{EMI}(10^{-20}\ cm^2)$
$^4S_{3/2}$	$//p$, 543.9	4.3	1.1
	$//m$, 543.9	3.8	0.9
	$//m$, 552.4	2.7	2.6
$^4I_{9/2}$	$//p$, 801.5	3.3	
	$//m$, 800.0	2.8	
	$//m$, 806.0	2.5	
$^4I_{11/2}$	$//p$, 981.0	5.1	
	$//m$, 978.2	5.7	

presented, the excitation was parallel to the principal p axis, but the emission shape does not change by exciting parallel to the principal m or g axes; however, the emission intensity is clearly related to the GSA intensity of the $^4S_{3/2}$ multiplet; see Fig. 2. Due to the low GSA of the $//g$ configuration, this excitation is less favourable for the up-conversion process and it will be ignored hereafter.

In a first approximation, the total area of the emission is little sensitive to the polarization state of the emitted light, i.e. the emission is weakly polarized. Several relative maxima are generally observed for the $^2H_{11/2} \rightarrow {}^4I_{15/2}$ transition at 522 nm, 525 nm, 527.6 nm, 531.2 ($//m, g$) nm, 532.4 ($//p$) nm and for the $^4S_{3/2} \rightarrow {}^4I_{15/2}$ one at 544 nm, 547.8 ($//p$) nm, 548.9 ($//m, g$) nm, 552.4 nm. It is worth remarking that the absolute maximum of the emission spectra related to the $^4S_{3/2}$ de-excitation shifts from 552.4 nm for light emitted parallel to the principal m and g axes to 544 and 547.8 nm for light emitted parallel to the principal p axis.

Figure 4 shows the excitation spectra of the green light emitted by an erbium-doped KGW crystal by up-conversion, either for the $^4I_{15/2} \rightarrow {}^4I_{11/2}$ excitation or for the $^4I_{15/2} \rightarrow {}^4I_{9/2}$ one. In both cases the excitation light is parallel to the principal p axis and the emission is recorded under unpolarized conditions. The figure includes for comparison the 300 K GSA polarized parallel to the p axis corresponding

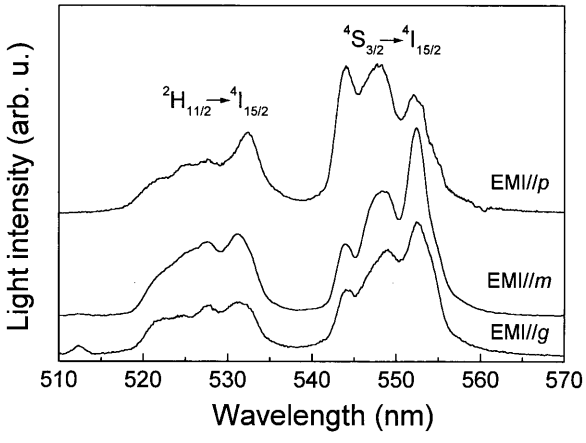

Fig. 3. 300 K polarized emission spectra excited by up-conversion in KGW:Er, [Er]$= 1.1 \times 10^{20}\ cm^{-3}$. The spectra are excited with light polarized parallel to the principal p axis at $\lambda_{EXC} = 801.5$ nm. Using $\lambda_{EXC} =$ 976.7 nm the results are similar. The analyzed polarizations are parallel to the principal axes of the indicatrix, labelled $//m$, $//g$ and $//p$

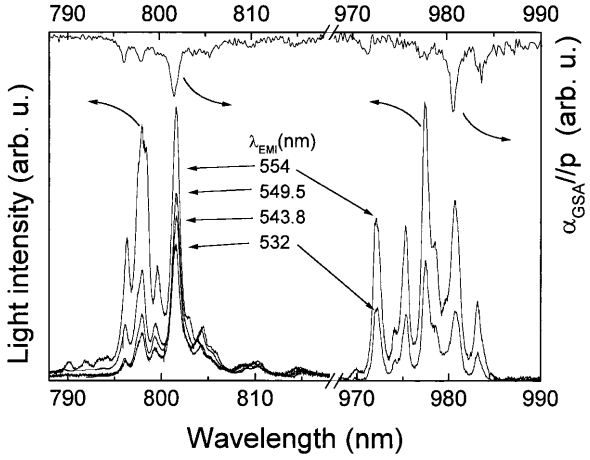

Fig. 4. 300 K excitation spectra of the green up-conversion in KGW:Er, [Er] $= 1.1 \times 10^{20}\ cm^{-3}$ for several relative maxima of the emission spectrum. The emission light is recorded unpolarized. The excitation is parallel to the principal p axis. The 300 K ground-state absorption, α_{GSA}, recorded parallel to the p axis for both multiplets, is given for comparison

to $^4I_{11/2}$ and $^4I_{9/2}$ multiplets. The excitation spectra of Fig. 4 show several peaks; the most intense ones are at 977.8 nm for the excitation at the $^4I_{11/2}$ multiplet and 798 and 801.5 nm for $^4I_{9/2}$ excitation. The spectral positions of these peaks and the GSA relative maxima agree for both multiplets. Small differences (< 1 nm) between the absorption and excitation are likely due to differences in the spectral calibration of the absorption and photoluminescence spectrometers. It is worth noting that for the $^4I_{11/2}$ multiplet the maximum excitation efficiency does not correspond to the maximum GSA. The shape of the excitation spectra for different emission wavelengths remains unchanged.

Figure 5a shows the intensity of the $^4S_{3/2} \rightarrow {}^4I_{15/2}$ emission induced by up-conversion for increasing Er concentrations. In the figure we have plotted the peak intensity at 552.4 nm for the available samples excited under identical experimental conditions. The excitation was parallel to the principal p axis and the emission includes contributions parallel to g and m. The peak intensity should have a maximum in the [Er] ≈ 1.5–$3 \times 10^{20}\ cm^{-3}$ range and decreases rapidly for larger Er concentrations.

Figure 5b shows the $^4S_{3/2}$ lifetime for KGW samples with increasing Er concentration. For the first three Er values used the decays are single-exponential or close to it; however, as the Er concentration exceeds $6 \times 10^{20}\ cm^{-3}$ non-exponential decays are clearly observed. The decays become faster as the Er concentration increases.

Figure 6a shows a logarithmic plot of the integrated up-conversion intensity (I_{EMI}) versus pumping intensity (I_{PUMP}) after excitation of the $^4I_{11/2}$ and $^4I_{9/2}$ multiplets respectively. These results can be empirically fitted by an $I_{EMI} = kI^s_{PUMP}$ law, k being a constant and s the slope of the straight line in the log–log plot. Within the experimental uncertainty and in the studied I_{PUMP} range, the results are well fitted using a straight line. Linear fits are also obtained in all samples considered. The slopes obtained depend very little on whether the $^2H_{11/2}$, $^4S_{3/2}$, or both decays are considered. Moreover, only little differences of the slope value are found for the emissions excited by pumping the $^4I_{11/2}$ or $^4I_{9/2}$ multiplets. Figure 6b shows the slopes obtained for different Er concentrations.

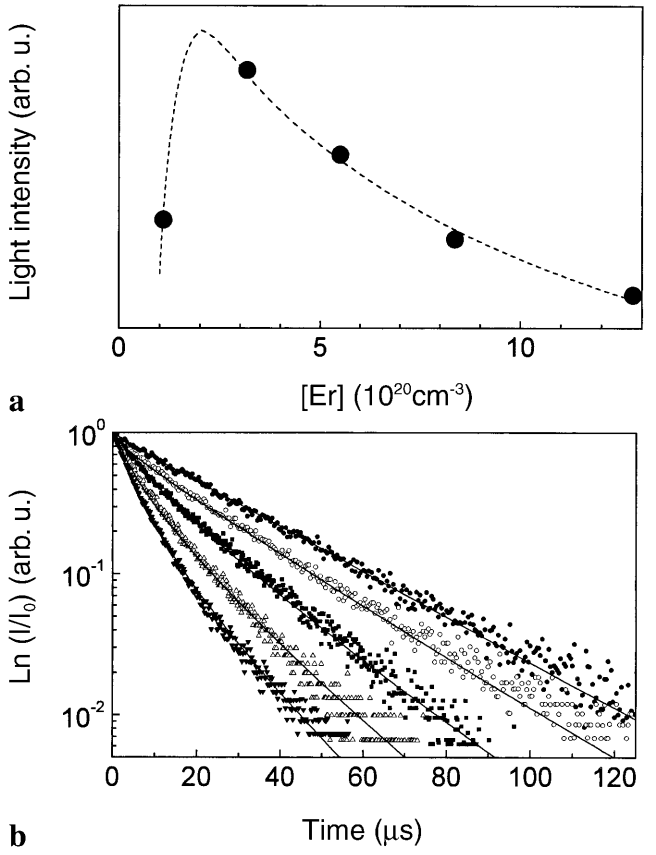

Fig. 5. a Evolution of the up-conversion intensity with the erbium concentration determined by PIXE. **b** 300 K lifetime of the $^4S_{3/2}$ multiplet for increasing Er concentration. ●, [Er] $= 1.1 \times 10^{20}$ cm^{-3}; ○, [Er]$= 3.1 \times 10^{20}$ cm^{-3}; ■, [Er]$= 5.5 \times 10^{20}$ cm^{-3}; △, [Er]$= 8.4 \times 10^{20}$ cm^{-3}; ▽, [Er]$= 12.8 \times 10^{20}$ cm^{-3}. The *points* are the experimental results and the *lines* are the fits obtained as described in the text

3 Discussion

Rare-earth impurities in KGW substitute Gd^{3+}; therefore the local symmetry point group, taking into account only the first oxygen neighbours, is C_2. The only symmetry element of this point group is a C_2 rotation axis parallel to the crystallographic *b* axis (i.e. the *p* axis of the indicatrix). According to this, ions such as Er^{3+} with semi-entire angular momentum *J* have two equivalent irreducible representations; therefore, no selection rules related to the polarization of the light are expected. The different GSA intensities observed in Fig. 2 arise from the differences in the transition-moment integral including the possible lattice–vibrational coupling.

The GSA of Er^{3+} measured with *g*-polarized light is generally the weakest; see Fig. 2. The GSA spectra corresponding to $//m$ and $//p$ light have similar intensities, although the spectral position of the maxima are not the same. These two pumping configurations were the best achieved, although the selection of the optimum polarization state for the green emission depends on the wavelength selected: while the $//m$ configuration is favourable for emission at $\lambda = 552.4$ nm, the $//p$ configuration is more efficient if $\lambda = 544$ or 547.8 nm were selected; see Fig. 3.

In Fig. 4 it can be observed that for a given pumping polarization configuration the intensity of the GSA and up-conversion excitation spectra are not linearly related, i.e. the spectral positions of the absolute maxima do not match. This is an indication that, at least for [Er] $\leq 3 \times 10^{20}$ cm^{-3}, the optical absorption of the excited states is the relevant excitation mechanism of the intermediate $^4I_{9/2}$ and $^4I_{13/2}$ multiplets. Therefore, energy cross-relaxation phenomena will be ignored.

Under this simplification, the whole efficiency of the up-conversion process for Er^{3+} is influenced by the absorption of the ground and excited states as well as by the emission efficiency of the $^4S_{3/2}$ level. In a previous work it was shown that the branching ratio for the $^4S_{3/2} \rightarrow {}^4I_{15/2}$ Er^{3+} transition in KGW is rather high, $\beta = 68\%$ [4]. Moreover, the emission cross section of this transition for a selected wavelength ($\lambda = c/\nu$), σ_{EMI}, can be obtained according to the reciprocity principle [15] as

$$\sigma_{\mathrm{EMI}} = \sigma_{\mathrm{GSA}} \frac{Z_{\mathrm{l}}}{Z_{\mathrm{u}}} \mathrm{e}^{(E_{\mathrm{zl}} - h\nu)/k_{\mathrm{B}}T} ,$$

where Z_{l} and Z_{u} are the partition functions of the lower and upper multiplets respectively and E_{zl} is the energy difference between the lowest Stark levels of these multiplets. Using the energy positions determined previously at 5 K [4] and the σ_{GSA} of the $^4S_{3/2}$ level given in Table 1,

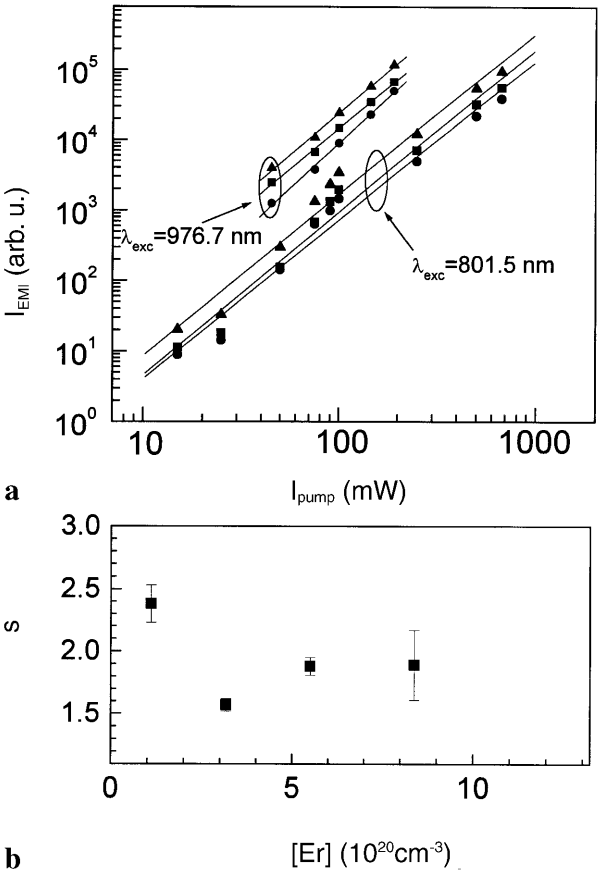

Fig. 6. a Logarithmic plots of the integrated up-conversion emission versus the pumping intensity at 300 K, [Er]$= 1.1 \times 10^{20}$ cm^{-3}. ●, $^2H_{11/2}$; ■, $^4S_{3/2}$ and ▲ , $^2H_{11/2}$+$^4S_{3/2}$. **b** Slope, *s*, of the $\log(I_{\mathrm{PUMP}}) - \log(I_{\mathrm{EMI}})$ representations as a function of the erbium concentration determined by PIXE

we have calculated the emission cross sections for several polarization/wavelength schemes. It is remarkable that some of the σ_{EMI} values obtained are as good as that found in the reference material $YLiF_4$, namely $2.0 \times 10^{20}\,cm^2$ [13]. Nevertheless, non-radiative losses are higher in KGW, i.e. for the lowest erbium concentration the 300 K $^4S_{3/2}$ fluorescence lifetime is 27 μs while the calculated radiative lifetime is 758 μs [4], this being detrimental for the final up-conversion efficiency.

In order to optimize the green output of light produced by up-conversion, in addition to the knowledge of the proper optical conditions (polarization and wavelength) for pumping, the optimum Er concentration must be determined. Figure 5a shows that maximum light output is achieved with $[Er] \approx 1.5\text{–}3 \times 10^{20}\,cm^{-3}$. The decrease of the photoluminescence intensity for Er concentrations above this limit is related to energy transfer between Er neighbours. This is quite clear from the behaviour of the $^4S_{3/2}$ lifetimes shown in Fig. 5b. For the two lowest Er concentrations used the decays are exponential; however, a clear departure from the exponential law is observed for $[Er] \geq 5 \times 10^{20}\,cm^{-3}$. The non-exponential decays have been analyzed by the Inokuti–Hirayama model [16], which provides the intensity decay for energy transfer to a continuous distribution of Er neighbours as

$$I(t) = I(0) \exp\left[\frac{-t}{\tau_0} - \Gamma\left(1 - \frac{3}{s}\right)\frac{[Er]}{c_0}\left(\frac{t}{\tau_0}\right)^{3/s}\right],$$

where $c_0 = 3/4\pi R_c^3$ is a critical concentration related to the R_c distance at which the donor-trap energy-transfer rate equals the spontaneous-decay rate and $s = 6$, 8 or 10 correspond to transfer mechanisms of electric dipole–dipole, dipole–quadrupole or quadrupole–quadrupole character respectively.

The continuous lines of Fig. 5b show the fits obtained using the lifetime of the lowest erbium concentration, $\tau_0 = 27\,\mu s$, $s = 6$ and assuming $R_c = 0.65 \pm 0.5\,nm$. This distance can be compared with the average Er–Er distance, $r = (4\pi[Er]/3)^{-1/3}$, which for $[Er] \geq 5.5 \times 10^{20}\,cm^{-3}$ yields $r \leq 0.75\,nm$. The comparison between the R_c and r distances indicates that for erbium concentrations higher than $5.5 \times 10^{20}\,cm^{-3}$, energy transfer between erbium donors and acceptors is very efficient, and responsible for the observed decrease of the $^4S_{3/2}$ photoluminescence yield.

Up-conversion is achieved by excitation of electrons in the intermediate $^4I_{11/2}$ and $^4I_{9/2}$ multiplets to higher energy levels. Photon absorption in the intermediate levels or energy transfer from excited Er^{3+} neighbours are the usual population mechanisms for the high energy levels. In the limit that the population of the intermediate levels is mainly controlled by the spontaneous decay to the lower-lying energy one, the intensity of the up-conversion emission depends on the absorbed light intensity as $I_{up} \approx I^n$, n being the number of photons involved in the excitation from the ground to the highest energy level [17]. High excitation of the intermediate levels, either by photon absorption or energy transfer, induces a decrease of n. The slopes found for $[Er] \geq 3.3 \times 10^{20}\,cm^{-3}$ samples are lower than 2 but close to this value. This suggests that at the erbium concentrations of interest for practical up-conversion, two-photon excitation is the most likely mechanism feeding the $^4S_{3/2}$ multiplet. Figure 1 sketches the most likely excitation paths. Even though the $^4I_{9/2}$ multiplet is directly pumped, this level is thermally bleached because of the low energy gap ($\approx 2100\,cm^{-1}$) to the lower-lying $^4I_{11/2}$ one, since the non-radiative decay probabilities depend on the energy gap between a populated level and the immediately lower-lying one. Also a depopulation of the $^4I_{11/2}$ multiplet to the $^4I_{13/2}$ one is expected, although to a lesser extent because of the larger energy gap between these two multiplets ($\approx 3450\,cm^{-1}$). A second electron photoexcitation from the $^4I_{13/2}$ multiplet is rather likely because of the large gap ($\approx 6150\,cm^{-1}$) to the $^4I_{15/2}$ multiplet, which minimizes non-radiative losses of thermal origin.

Figure 6b shows that the slope of the $\log(I_{EMI})$–$\log(I_{PUMP})$ plots obtained in the sample with lowest erbium concentration ($[Er] = 1.1 \times 10^{20}\,cm^{-3}$) is clearly higher than 2, either if the $^4I_{11/2}$ or the $^4I_{9/2}$ multiplets are excited. This result would indicate that for this particular concentration three photons of either 976.7 nm or 801.5 nm would be involved in the Er^{3+} up-conversion process in KGW. Three-photon excitation of the up-conversion in Er^{3+} has been reported in fluorides [9, 18] and lead-germanate glass [19]. In these cases ultraviolet, violet and blue up-conversion photoluminescence due to the $^3P_{3/2}$, $^4G_{11/2}$ and $^2H_{9/2}$ decays are observed. Such emissions were not found in our KGW:Er lowest concentration sample. This difference may be due to the much broader phonon spectrum of KGW with regard to fluorides. For the $^4G_{11/2}$ and $^2H_{9/2}$ multiplets of Er^{3+} in KGW these gaps are about 1617 and $1945\,cm^{-1}$ respectively [4]. As the cut-off phonon frequency for KGW is $901\,cm^{-1}$ only the emission of two phonons would be required for a non-radiative decay. This compares with fluorides (BaF_2 and LaF_3) where the maximum phonon energy is about $350\,cm^{-1}$ and therefore up to six phonons should be required, making the radiative process more likely than in KGW. The gap is higher for the $^3P_{3/2}$ multiplet ($\approx 3400\,cm^{-1}$) and the ultraviolet ($\approx$ 315–325 nm) emission of the $^3P_{3/2}$ multiplet is likely to occur. Unfortunately, this is outside the spectral response of our detector. Anyhow, this emission could be difficult to observe since it could be partially reabsorbed by the KGW matrix having a 300 K optical absorption threshold of ≈ 291 nm [20].

The different slopes found between the lowest concentration sample and the rest of the concentrations used could be related to an efficient energy migration of the uppermost energy levels.

4 Conclusions

Room-temperature Er^{3+} up-conversion in KGW crystals was achieved by exciting the $^4I_{11/2}$ or $^4I_{9/2}$ multiplets. The $^4S_{3/2} \rightarrow {}^4I_{15/2}$ Er^{3+} emission efficiency is similar and even higher than other currently used materials. Pumping with light polarized parallel to m ($\lambda = 978.2$ and 800 nm) or p ($\lambda = 981$ and 801 nm) axes of the indicatrix and using an erbium concentration in the range $[Er] \approx 1.5\text{–}3 \times 10^{20}\,cm^{-3}$ optimize the up-conversion emission intensity. The green emissions are weakly polarized. Under these conditions, a two-photon excitation process is suggested, although a more complex process may happen for the lowest concentration used.

Acknowledgements. This work is supported by CICyT under projects 2FD97-0912 and MAT99-1077.

References

1. A.A. Demidovich, A.P. Shkadarevich, M.B. Danailov, P. Apai, T. Gasmi, V.P. Gribkovskii, A.N. Kuzmin, G.I. Ryabtsev, L.E. Batay: Appl. Phys. B **67**, 11 (1998)
2. A.A. Kaminskii, H. Nishioka, Y. Kubota, K. Ueda, H. Takuma, S.N. Bagaev, A.A. Pavlyuk: Phys. Stat. Sol. (a) **148**, 619 (1995)
3. A.A. Kaminskii, K. Ueda, H.E. Eichler, J. Findeisen, S. Bagayev, F.A. Kuznetsov, A.A. Pavlyuk, G. Boulon, F. Bourgeois: Jpn. J. Appl. Phys. **37**, L923 (1998)
4. M.C. Pujol, M. Rico, C. Zaldo, R. Solé, V. Nikolov, X. Solans, M. Aguiló, F. Díaz: Appl. Phys. B **68**, 187 (1999)
5. L.I. Yudanova, A.A. Pauyuk, O.G. Potapova: Neorg. Mat. **28**, 2208 (1992)
6. J. Thogersen, N. Bjerre, J. Mark: Opt. Lett. **18**, 197 (1993)
7. T. Honda, T. Doumuki, A. Akella, L. Galambos, L. Hesselink: Opt. Lett. **23**, 1108 (1998)
8. T. Danger, J. Koetke, R. Brede, E. Heumann, G. Huber, B.H.T. Chai: J. Appl. Phys. **1413**, 76 (1994)
9. B.R. Reddy, S.K. Nash-Stevenson: J. Appl. Phys. **76**, 3896 (1994)
10. A.J. Silversmith, W. Lenth, R.M. Macfarlane: Appl. Phys. Lett. **51**, 1977 (1987)
11. F. Heine, E. Heumann, T. Danger, T. Schweizer, G. Huber, B. Chai: Appl. Phys. Lett. **65**, 383 (1994)
12. R. Brede, E. Heumann, J. Koetke, T. Danger, H. Huber, B. Chai: Appl. Phys. Lett. **63**, 2030 (1993)
13. P. E.-A. Möbert, E. Heumann, G. Huber, B.H.T. Chai: Opt. Lett. **22**, 1412 (1997)
14. L. Núñez, G. Lifante, F. Cussó: Appl. Phys. B **62**, 485 (1996)
15. D.E. McCumber: Phys. Rev. **136**, 954 (1964)
16. M. Inokuti, F. Hirayama: J. Chem. Phys. **43**, 1978 (1965)
17. M. Pollnau, D.R. Gamelin, S.R. Lüthi, H.U. Güdel, M.P. Hehlen: Phys. Rev. B **61**, 3337 (2000)
18. D.N. Patel, R.B. Reddy, S.K. Nash-Stevenson: Appl. Opt. **37**, 7805 (1998)
19. Z. Pan, S.H. Morgan, A. Loper, V. King, B.H. Long, W.E. Collins: J. Appl. Phys. **77**, 4688 (1995)
20. M.C. Pujol, R. Solé, Jna. Gavaldá, J. Massons, M. Aguiló, F. Díaz, V. Nikolov, C. Zaldo: J. Mater. Res. **14**, 3739 (1999)